ORIGINAL ARTICLE

JBMR

Cyr61 Expression in Osteosarcoma Indicates Poor Prognosis and Promotes Intratibial Growth and Lung Metastasis in Mice

Adam A Sabile,[1] Matthias JE Arlt,[1] Roman Muff,[1] Beata Bode,[2] Bettina Langsam,[1] Josefine Bertz,[1] Thorsten Jentzsch,[1] Gabor J Puskas,[1] Walter Born,[1] and Bruno Fuchs[1]

[1]Laboratory for Orthopedic Research, Department of Orthopedics, Balgrist University Hospital, Zurich, Switzerland
[2]Institute of Surgical Pathology, University Hospital, Zurich, Switzerland

ABSTRACT

Osteosarcoma is the most frequent primary malignant bone tumor in children and adolescents with a high propensity for lung metastasis, the major cause of disease-related death. Reliable outcome-predictive markers and targets for osteosarcoma metastasis-suppressing drugs are urgently needed for more effective treatment of metastasizing osteosarcoma, which has a current mean 5-year survival rate of approximately 20%. This study investigated the prognostic value and the biological relevance of the extracellular matrix-associated growth factor Cyr61 of the CCN family of secreted proteins in osteosarcoma and metastasis. The prognostic value of Cyr61 was assessed with Kaplan-Meier analyses based on Cyr61 immunostaining of a tissue microarray of osteosarcoma biopsies collected from 60 patients with local or metastatic disease. Effects of Cyr61 overexpression on intratibial tumor growth and lung metastasis of the low metastatic human SaOS-2 osteosarcoma cell line were examined in severe combined immunodeficiency (SCID) mice. Cyr61-provoked signaling was studied in vitro in nonmanipulated SaOS-2 cells. Cyr61 immunostaining of osteosarcoma tissue cores correlated significantly ($p = 0.02$) with poor patient survival. Mice intratibially injected with Cyr61-overexpressing SaOS-2 cells showed faster tumor growth and an increase in number and outgrowth of lung metastases and consequently significantly ($p = 0.0018$) shorter survival than mice injected with control SaOS-2 cells. Cyr61-evoked PI-3K/Akt/GSK3β signaling in SaOS-2 cells resulted in a subcellular redistribution of the cell cycle inhibitor $p21^{Cip1/WAF1}$. Cyr61 has considerable potential as a novel marker for poor prognosis in osteosarcoma and is an attractive target for primary tumor- and metastases-suppressing drugs. © 2012 American Society for Bone and Mineral Research.

KEY WORDS: OSTEOSARCOMA; METASTASIS; CYR61; TISSUE MICROARRAY; MOUSE MODEL

Introduction

Osteosarcoma is the most common primary malignant bone tumor in children and young adults with a high propensity for metastasis, predominantly to the lung, and consequently is associated with poor prognosis.[1–3] Multiagent neoadjuvant chemotherapy combined with primary tumor resection increased the mean 5-year survival rate of osteosarcoma patients with localized disease from 20% to 70%. In contrast, patients who present with metastases at diagnosis continue to have a poor prognosis, reflected by a mean 5-year survival of approximately 20%.[4–6] Histological grading of tumor biopsies and evaluation of the necrosis rate in the resected tumor after chemotherapy are routinely used as predictors for the survival of osteosarcoma patients. However, reliable and robust diagnostic and prognostic markers, described for other tumor types, hardly exist in osteosarcoma. Among the candidate proteins considered to have particular biological relevance in osteosarcoma, the cytoskeletal linker protein ezrin is the best characterized protein with potential diagnostic and prognostic relevance in osteosarcoma.[7–10] A better understanding of the heterogeneity and complexity of osteosarcoma pathophysiology and metastasis, which is still needed to further improve the diagnosis and treatment of this devastating disease, requires the identification and detailed characterization of so far unknown regulators of osteosarcoma and metastasis progression. Here, the cysteine-rich protein Cyr61 (CCN1), based on its tumor- and metastasis-promoting activity in many tumor types, was considered as a novel prognostic marker and therapeutic target in osteosarcoma.

Received in original form April 21, 2011; revised form August 2, 2011; accepted August 29, 2011. Published online October 4, 2011.
Address correspondence to: Bruno Fuchs, MD, PhD, Laboratory of Orthopedic Research, Balgrist University Hospital, Forchstrasse 340, CH-8008 Zurich, Switzerland. E-mail: bfuchs@research.balgrist.ch
Additional Supporting Information may be found in the online version of this article.

Journal of Bone and Mineral Research, Vol. 27, No. 1, January 2012, pp 58–67
DOI: 10.1002/jbmr.535

Cyr61 belongs to the CCN family of six structurally related proteins. It has attracted considerable interest in cancer research because of its regulatory functions in several processes relevant in tumor biology including cell adhesion, migration, proliferation, differentiation, angiogenesis, apoptosis, and survival.[11–16] In breast cancer, Cyr61 was found to be expressed at higher levels in tumors than in normal breast tissue, and increased expression correlated with tumor size, involvement of lymph nodes, and metastatic potential of tumor cells and consequently poor survival.[17–19] In glioma, Cyr61 was found overexpressed in primary tumors compared with normal tissue, and its expression levels correlated significantly with tumor grade and inversely with patient survival.[20] Cyr61 was also shown to promote the growth of glioma cells.[21] Cyr61 was found upregulated in colon adenoma, pancreatic cancer, and glioblastoma.[22] Forced expression of Cyr61 in ovarian cancer increased tumorigenicity and accelerated tumor growth in nude mice, whereas inhibition of Cyr61 expression in ovarian cancer cells decreased the proliferation rate and enhanced apoptosis.[23] In other tumors such as endometrial, gastric, and lung cancers, the tumor- and metastasis-promoting activity of Cyr61 is still under debate.[24–29] A recent study in an intramuscular spontaneously metastasizing mouse osteosarcoma model demonstrated that shRNA-mediated downregulation of Cyr61 inhibited lung metastasis.[30] This suggested a metastatic-promoting activity of Cyr61 in osteosarcoma, which was confirmed in the same study in human osteosarcoma cell lines in vitro and upon overexpression in the mouse model. These findings in experimental mouse osteosarcoma were consistent with the data of an immunohistochemical analysis of human osteosarcoma tissue, which showed that Cyr61 expression increased with tumor grade.

The current study demonstrates that expression of Cyr61 in osteosarcoma biopsies correlates with poor survival of the patients, irrespective of metastatic or nonmetastatic disease. Moreover, experiments in a remarkably precise intratibial model of human metastasizing osteosarcoma in severe combined immunodeficiency (SCID) mice showed that forced overexpression of Cyr61 in the low-metastatic human SaOS-2 osteosarcoma cell line accelerated the growth of intratibial xenografts and promoted lung metastasis. Altogether, the results reported here point to a great potential of Cyr61 as a novel diagnostic marker and therapeutic target in osteosarcoma.

Materials and Methods

Human osteosarcoma tissue array, Cyr61 immunostaining, and Kaplan-Meier analysis

Primary osteosarcoma biopsies of 60 patients and normal bone tissue specimens were collected between June 1990 and December 2005 according to the regulations of the local ethical committee. Osteosarcoma patients had a mean follow-up of 83 months (range 10 to 213 months). A database containing information on basic demographics, patient survival, anatomic location, response to chemotherapy, type of resection, surgical margin, occurrence and timing of metastasis, as well as local recurrence was established by a retrospective chart review. The patients included 21 (35%) females and 39 (65%) males. Tumor tissue specimens were histologically reevaluated and grouped into subtypes according to the current histopathological classification of bone tumors.[31] Tumors were osteoblastic in 41 (68%) patients, chondroblastic in 10 (17%) patients, fibroblastic in 5 (8%) patients, and telangiectatic in 4 (7%) patients. Fifty (83%) patients presented with tumors in an extremity, and 10 (17%) patients suffered from an axial tumor (pelvis or spine). Metastases were detected in 22 (37%) patients, and 5 (10%) of these patients presented with metastases at diagnosis. The lungs were a sole metastatic site in 18 (82%) patients, lung and bone metastases were found in 3 (14%) patients, and the metastatic site was not known in 1 (5%) patient. Six patients (10%) had local recurrence.

Biopsies with histologically confirmed non-necrotic tumor tissue from surgical specimen were marked, and two tissue cores per tumor and normal bone specimens with a diameter of 0.6 mm were arranged in a tissue array as described.[32] A 4.5-μm section of the tissue array was transferred to an adhesive-coated slide system (Instrumedics, Hackensack, NJ, USA), deparaffinized, and processed with a Bond Automated Staining System (Vision BioSystems, Newcastle, UK). After antigen retrieval in EDTA containing buffer (Bond Epitope Retrieval Solution 2; Vision BioSystems) for 30 minutes, the section was stained with Cyr61 antibodies (1:400) (Santa Cruz Biotechnology, Santa Cruz, CA, USA) and counterstained with hematoxylin. A Kaplan-Meier analysis correlated Cyr61 immunostaining with overall survival of patients with and without metastatic disease.

Cell culture and transfection

Human SaOS-2 osteosarcoma cells (HTB-85) purchased from American Type Culture Collection (ATCC; Manassas, VA, USA) were cultured in Dulbecco's modified Eagle medium (4.5 g/L glucose; Gibco, Invitrogen, Carlsbad, CA, USA) and Ham F12 medium (Gibco) (1:1), supplemented with 10% heat-inactivated fetal calf serum (FCS; Invitrogen) at 37°C in a humidified atmosphere of 5% CO_2. SaOS-2 cells stably overexpressing N-terminally myc-tagged Cyr61 (SaOS-2/Cyr61 cells) were obtained by calcium phosphate precipitation-mediated transfection[33] with the pcDNA3-neo-derived plasmid pMyc-Cyr61 and selection for neomycin resistance with 500 μg/mL G418 (Invitrogen). Control pcDNA3-neo-transfected SaOS-2 (SaSO-2/EV) cells were obtained accordingly.

Wound-healing migration assay

Cells were seeded in 24-well plates (six wells per assay) and at confluence, and wounds of 0.8 to 1 mm in width and approximately 1 cm in length were created with a sterile pin, inspected, and measured immediately after wounding under a Nikon Diaphot (Nikon Corp., Tokyo, Japan) microscope with a 1-mm-scale graded ocular. Homogenous wound areas free of cell debris were marked using a round Nikon object marker, and the width of the wounds were measured in the center of the marked area. After incubation at 37°C for 16 hours, the cells were fixed with 10% formalin at room temperature for 15 minutes and washed twice with PBS. The widths of the marked wounds were then measured again and the cell migration velocity (μm/hour) calculated.

Boyden chamber migration and invasion assays

In vitro migration and invasion were assessed in BD Falcon (BD Biosciences, San Jose, CA, USA) cell culture inserts (growth area 0.3 cm^2; pore size 8 μm). A total of 2×10^4 cells in 300 μl serum-free cell culture medium were seeded in the upper compartment, and 700 μl of cell culture medium with 10% fetal calf serum (FCS) were applied to the lower compartment of a 24-well companion plate. For cell invasion experiments, the inserts were coated with 12 μg Matrigel (40 $\mu g/cm^2$; BD Biosciences) in 100 μl serum-free medium by air-drying overnight. The number of migrating or invading cells was determined 48 hours after cell seeding. Cells in the upper compartment were removed with a cotton bud and those in the lower compartment fixed with 10% formalin at room temperature for 15 minutes, permeabilized with 50 μM digitonin in PBS, and the nuclei stained with PicoGreen (Molecular Probes, Invitrogen; 1:300) at room temperature for 15 minutes. Cell nuclei were counted with ImageJ software (http://rsb.info.nih.gov/ij/) in four randomly selected areas of 3.6 mm^2 of images obtained with a Zeiss Observer.Z1 (Zeiss, Inc., Thornwood, NY, USA) fluorescence microscope equipped with an objective of ×4 magnification and a Zeiss AxioCam MRm (Zeiss, Inc.) camera. The invasion indexes were calculated from the number of cells migrating within 48 hours across Matrigel-coated filters divided by the number of cells migrating in the same time period across noncoated filters.

Intratibial human osteosarcoma xenograft mouse model

Eight-week-old female SCID mice were obtained from Charles River Laboratories (Wilmington, MA, USA) at least 10 days before experimental commencement. Housing conditions and experimental protocols were in accordance with the guidelines of the "Schweizer Bundesamt für Veterinärwesen" and approved by the local authorities. For tumor cell injection, the mice were anesthetized with Fentanyl (Sintenyl, Sintetica SA, Mendrisio, Switzerland), Midazolam (Dormicum, Roche Pharma, Basel, Switzerland), and Medetomidin (Dorbene, Graeub Veterinary Products, Bern, Switzerland). A total of 5×10^5 SaOS-2/EV or SaOS-2/Cyr61 cells in 10 μl PBS were then injected intramedullary with a Hamilton syringe into the left tibia of individual mice under X-ray control with a MX-20 DC Digital Radiography System (Faxitron X-Ray Corporation, Lincolnshire, IL, USA). The health status of the mice was monitored three times a week and primary tumor growth examined in 2-week intervals by X-ray and by calculating the tumor volume with the equation length × $(width)^2/2$ of the tumor-bearing tibia minus length × $(width)^2/2$ of the control tibia after measurements of the respective widths and the lengths with a caliper. We performed two experiments. In the first experiment, mice were sacrificed individually when they became moribund (time course/survival study). In the second experiment, all mice were sacrificed on the same day when the first mouse in the group injected with Cyr61-overexpressing cells became moribund (endpoint experiment).

Histology of lung metastases

On the day of sacrifice, the mice were anesthetized with Ketamine (Narketan 10, Vétoquinol AG, Bern, Switzerland), Xylazine (Streuli Pharma AG, Uznach, Switzerland), and Acepromazine (Prequilan, Fatro SpA, Ozzano Emilia, Italy), and the thorax and abdomen were opened. Blood was removed from the lungs and the liver by PBS perfusion into the right ventricle of the beating heart. The lungs were fixed for 10 minutes with 3% paraformaldehyde (PFA) injected into the right ventricle and into the trachea with subsequent pinch-off. Lungs and tumor-bearing legs were removed and subjected to additional fixation with 4% PFA in PBS. PFA-fixed lungs were embedded into paraffin, and 5-μm sections were obtained with a Leica RM2155 microtome (Leica Biosystems, Heerbrugg, Switzerland). Ten sections per lung at 200-μm intervals were collected, mounted on SuperFrost Plus slides (Menzel GmbH & Co KG, Braunschweig, Germany), and processed for hematoxylin-eosin (HE) staining according to standard protocols. Metastatic nodules per section were counted under an Eclipse E600 microscope (Nikon Corp.), and the mean number of lung lesions per sagittal section was then calculated.

Analysis of Cyr61 signaling in SaOS-2 cells

Cells seeded at 50% confluence, grown for 24 hours, and serum-starved for 48 hours were stimulated for 30 minutes with human recombinant (hr)Cyr61 at indicated concentrations in the absence or in the presence of 100 μM PI-3K inhibitor LY294002 (Cell Signaling Technology, Danvers, MA, USA), or of the Gly-Arg-Gly-Asp-Ser (GRGDS) integrin blocking peptide or the Ser-Asp-Gly-Arg-Gly (SDGRG) control peptide (Sigma, St. Louis, MO, USA), or of the blocking antibodies to αVβ3, αVβ5, and α5β1 integrins (Millipore, Billerica, MA, USA). They were then lysed in ice-cold 50 mM Tris, pH 7.5 containing 250 mM NaCl, 5 mM EDTA, 0.5% NP-40, 50 mM NaF, 0.2 mM Na_3VO_4, 1 mM dithiothreitol (DTT), 1 mM phenylmethylsulphonyl fluoride (PMSF), and 10 μg/ml aprotinin. Cell lysates were cleared by centrifugation at 45,000 *g* at 4°C for 30 minutes and protein concentrations determined with a Bio-Rad assay (Bio-Rad Laboratories, Hercules, CA, USA).

Cytoplasmic and nuclear fractions were obtained from cells harvested in ice-cold PBS, washed three times in 10 mM HEPES, pH 7.9, containing 1.5 mM $MgCl_2$, 10 mM KCl, 1 mM DTT and phenylmethylsulfonyl fluoride (PMSF), leupeptin, aprotinin, and pepstatin (buffer A), and then lysed in 150 μl buffer A supplemented with 0.1% NP-40. Cell lysates were cleared by centrifugation at 5000 *g* for 5 minutes at 4°C and the supernatant cytoplasmic fractions collected. Nuclear pellets were washed twice with buffer A and extracted by gentle rocking at 4°C for 20 minutes in 150 μl 20 mM HEPES, pH 7.9, containing 1.5 mM $MgCl_2$, 0.42 M NaCl, 25% glycerol, 1 mM DTT and PMSF, leupeptin, aprotinin, and pepstatin. Extracts were centrifuged at 10,000 *g* for 5 minutes at 4°C and the supernatant nuclear fractions collected.

Cyr61-regulated signaling proteins in total cell lysates and cytoplasmic and nuclear fractions were analyzed on Western blots after separation by SDS-PAGE of 50 μg total protein of individual fractions and semidry blotting to nitrocellulose

membranes. The proteins analyzed with corresponding antibodies included human Cyr61 and proliferating cell nuclear antigen (PCNA; Santa Cruz Biotechnology), the myc-epitope tag and β-actin (Millipore), phospho-Akt, Akt, phospho-GSK-3β, GSK-3β, the cell cycle inhibitor p21, and Cyclin D1 (Cell Signaling Technology). Proteins were visualized by enhanced chemoluminescence (ECL) with horseradish peroxidase (HRP)-labeled secondary antibodies (Molecular Probes) and detected with a VersaDoc imaging system and quantified with Quantity One software (Bio-Rad Laboratories).

Statistical analysis

Results are presented as mean ± standard error of the mean (SEM). Differences between means were analyzed for significance by unpaired *t* test with GraphPad Prism 5.01 software (GraphPad Software, La Jolla, CA, USA). Overall patient survival was calculated using Kaplan-Meier curves with assessment of statistical significance using the log-rank test. A p value ≤ 0.05 was considered statistically significant.

Results

Expression of Cyr61 in human osteosarcoma tissue correlates with poor survival of the patients

Cyr61 immunohistochemistry was performed as outlined in Materials and Methods on an osteosarcoma tissue microarray, consisting of tissue cores of primary tumors collected from 60 patients with a mean age of 22 years (range 2 to 66 years) (Fig. 1*A, B*). Twenty-two patients had metastatic disease, and 5 of them presented with metastases at diagnosis. A Kaplan-Meier survival analysis showed that, irrespective of metastatic or local disease, 37 patients with immunohistochemically detectable expression of Cyr61 in tumor tissue had a significantly ($p = 0.02$) shorter overall survival of 92 ± 9 (mean ± SE) months than 23 patients with nondetectable Cyr61 expression and a mean overall survival of 189 ± 13 months (Fig. 1*C*). A second Kaplan-Meier survival analysis, which, in addition to nondetectable or detectable expression of Cyr61, distinguished between patients with local or with metastatic disease, revealed the shortest survival time of 47 ± 9 months for 17 patients with metastases and detectable expression of Cyr61 in the primary tumor (Fig. 1*D*). Interestingly, patients with metastatic disease but nondetectable Cyr61 expression ($n = 5$) had a considerably longer mean survival time of 123 ± 30 months. Thus, Cyr61 expression in primary tumor tissue appears to significantly affect the aggressiveness of osteosarcoma. Accordingly, even patients with only local disease and Cyr61-expressing tumors tended to have a shorter survival than those with Cyr61-negative tumors.

Overexpression of Cyr61 in the human low-metastatic SaOS-2 osteosarcoma cell line increases the migration rate and the invasive activity in vitro

Based on the results of the Kaplan-Meier analyses, we speculated that Cyr61 expressed by the primary tumor may be a stimulatory

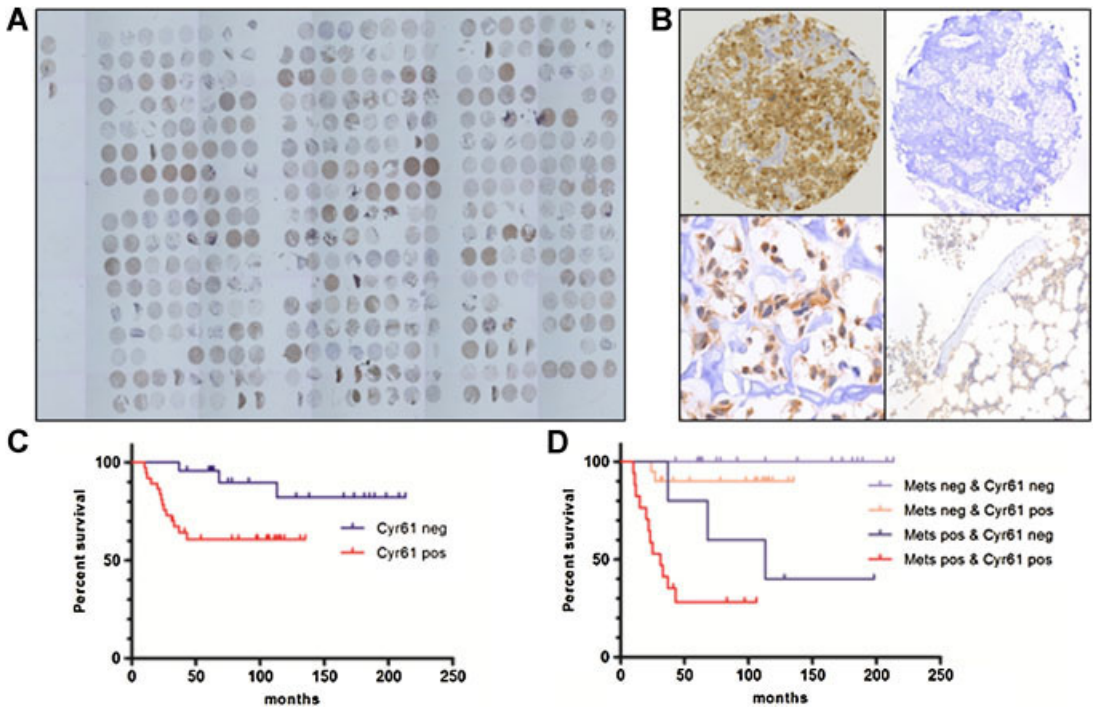

Fig. 1. Cyr61 immunohistochemical staining of human osteosarcoma tissue biopsies correlates with poor patient survival. (*A*) Cyr61 immunostaining (brown) of a tissue microarray consisting of control normal bone tissue and of specimens from osteosarcoma biopsies. (*B*) Cyr61 immunostaining of a randomly selected representative tumor specimen (top left) and nonspecific control staining of a corresponding tissue specimen in the absence of primary Cyr61 antibodies (top right). Representative high-power magnification of tumor tissue (bottom left) and of normal bone (bottom right) immunostained for Cyr61. (*C, D*) Kaplan-Meier survival analysis indicating overall survival of osteosarcoma patients with nondetectable (Cyr61 neg) or detectable (Cyr61 pos) Cyr61 immunostaining in tumor biopsies (*C*) and of patients without (Mets neg) or with (Mets pos) metastases and Cyr61 neg or Cyr61 pos primary tumors (*D*).

factor in the regulation of metastatic activity of tumor cells. Consequently, we compared wound-healing migration and the capability for Matrigel invasion of SaOS-2 cells stably overexpressing myc-tagged Cyr61 (SaOS-2/Cyr61) with that of empty vector transfected SaOS-2 (SaOS-2/EV) control cells with low expression of endogenous Cyr61. The levels of myc-Cyr61 expression in SaOS-2/Cyr61 cells were at least 5 times higher than those of endogenous Cyr61 (Fig. 2*A*). The migration rate of SaOS-2/Cyr61 cells was 2.5 times ($p < 0.0002$) higher than that of control SaOS-2/EV cells (Fig. 2*B*). The rate of invasion of Matrigel by SaOS-2/Cyr61 cells, indicated by a calculated invasion index, was 1.7-fold higher ($p < 0.04$) than that of SaOS-2/EV cells (Fig. 2*C*). The number of SaOS-2/Cyr61 and SaOS-2/EV cells migrating across noncoated filters amounted to $31 \pm 9\%$ and $21 \pm 8\%$ ($p > 0.05$) of the respective seeded cells. It is noteworthy that overexpression of Cyr61 did not affect the proliferation of SaOS-2 cells in vitro. The calculated doubling times and the percentage of proliferating cells, assessed by immunostaining for the proliferation marker Ki67, were indistinguishable in cultures of SaOS-2/Cyr61 and SaOS-2/EV cells (not shown).

Cyr61 promotes intratibial primary tumor growth and lung metastasis in mice

The results of the in vitro migration and invasion studies pointed to an increased metastatic potential of Cyr61-overexpressing SaOS-2/Cyr61 cells compared with control SaOS-2/EV cells. Consequently, primary tumor formation and metastasis to the lung of SaOS-2/Cyr61 and of SaOS-2/EV cells were compared in an intratibial xenograft osteosarcoma model in SCID mice. SaOS-2/Cyr61 or control SaOS-2/EV cells were injected orthotopically into the medulla of the left tibia of the mice (Fig. 3*A*). Four of five mice injected with SaOS-2/Cyr61 cells developed primary tumors that were visible on X-ray on day 28 after tumor cell injection (Fig. 3*B*, lower panel). This was consistent with swelling of the tumor leg, first observed 21 days after tumor cell injection. In contrast, in all control mice injected with SaOS-2/EV cells, primary tumors remained radiologically undetectable until day 64 after tumor cell injection (Fig. 3*B*, upper panel), but all control mice developed visible tumors between day 64 and day 90 post-tumor cell inoculation. Leg swelling was also not observed in any of the control mice before day 64 after tumor cell injection. This suggested that tumors derived from SaOS-2/Cyr61 cells grew faster than those from SaOS-2/EV cells. However, immunohistochemical staining of tissue sections of respective tumors for the proliferation marker Ki67 revealed a comparable percentage of proliferating cells in SaOS-2/Cyr61 and SaOS-2/EV cell-derived tumors (not shown). All X-ray detectable tumors in the two groups of mice showed both osteolytic and osteoblastic lesions in the bone and the surrounding soft tissue (Fig. 3*B*). It is noteworthy that the mice injected with SaOS-2/Cyr61 cells became moribund and had to be sacrificed before the control mice developed measurable or radiologically visible primary tumors (Fig. 3*C*). Accordingly, Kaplan-Meier survival curves plotted for the mice in the two groups indicated a significantly ($p < 0.002$) shorter mean survival of the SaOS-2/Cyr61 cell-injected mice compared with control animals (Fig. 3*D*). Interestingly, at sacrifice the mean size of primary tumors in the SaOS-2/Cyr61 cell-injected mice was smaller than that in control animals, suggesting that the mice with SaOS-2/Cyr61 cell-derived tumors developed early and severe metastasis. This was confirmed by histological examination of HE-stained sections of the lungs. Although all SaOS-2/Cyr61 cell-injected mice were sacrificed at least 27 days before the sacrifice of the first mouse in the control group, they exhibited more and larger metastatic foci in their lungs than the control mice (data not shown). This was confirmed in a second study in which both the SaOS-2/Cyr61 cell-injected and the control mice were sacrificed on the same day when the first animals in the SaOS-2/Cyr61 group became moribund. In SaOS-2/Cyr61 cell-injected mice, the mean number of metastatic lesions per section was 1.7 times higher than that in control animals (Fig. 4*A*). Moreover, lung metastases observed in SaOS-2/Cyr61 cell-injected mice were larger than 1 mm in diameter (Fig. 4*B*). In contrast, none of the control mice had lung lesions larger than 1 mm in diameter. Taken together, Cyr61 overexpression enhances the malignancy of the low-metastatic SaOS-2 cells.

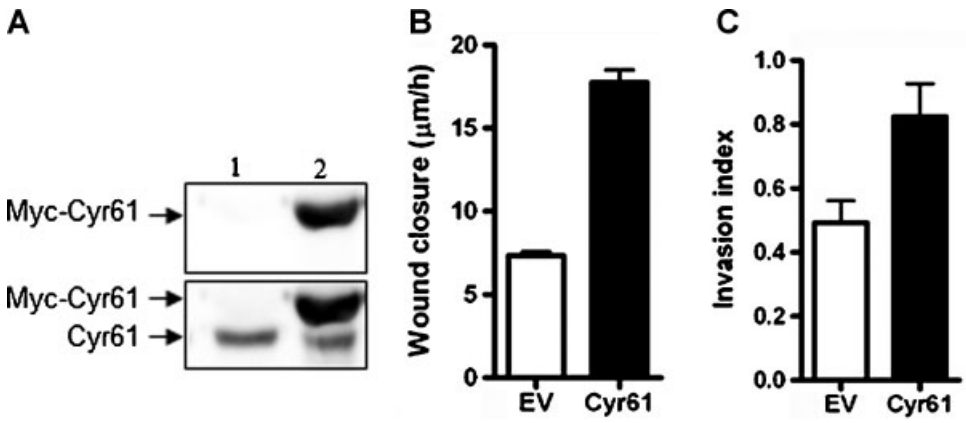

Fig. 2. Overexpression of Cyr61 in SaOS-2 cells increases migration and invasion activity. (*A*) Western blot analysis with antibodies to myc (top panel) and to Cyr61 (bottom panel) of protein extracts from SaOS-2 cells stably transfected with pcDNA3.1-neo (EV) (lane 1) or with pcDNA3.1-neo-derived pMyc-Cyr61 (lane 2). (*B*) Migration assessed by wound healing and (*C*) Matrigel invasion activity of SaOS-2/EV and SaOS-2/Cyr61 cells. Results in (*B*) and (*C*) are the mean ± SEM of at least three independent experiments.

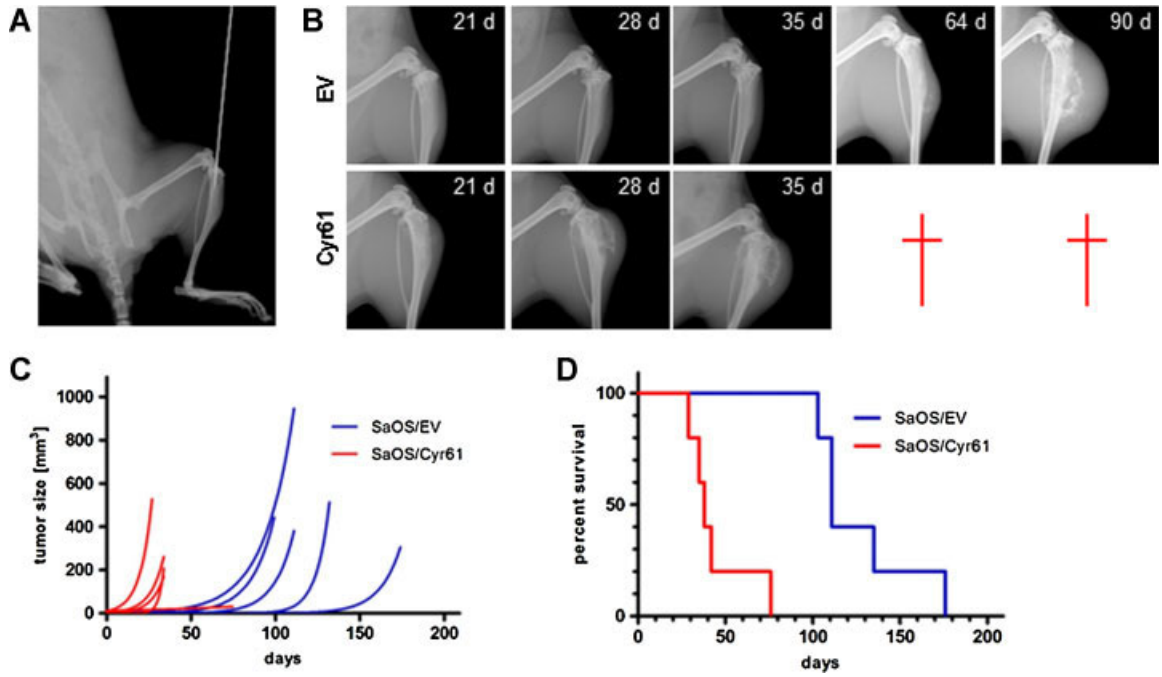

Fig. 3. Cyr61 overexpression in SaOS-2 osteosarcoma cells promotes intratibial primary tumor growth in SCID mice. (*A*) Representative X-ray control image of the position of the Hamilton syringe during intratibial injection of tumor cells. (*B*) Representative X-ray images of tumor-bearing hindlimbs of mice injected with SaOS-2/EV cells (top panels) or with SaOS-2/Cyr61 cells (bottom panels). The images show primary tumor appearance on indicated days after tumor cell injection. † = all mice injected with SaOS-2/Cyr61 cells had to be sacrificed before the indicated days. (*C*) Primary intratibial tumor growth over time in individual mice injected with SaOS2/EV cells (blue) or with SaOS-2/Cyr61 cells (red). (*D*) Kaplan-Meier survival analysis indicating overall survival of mice injected with SaOS2/EV cells (blue) or with SaOS-2/Cyr61 cells (red).

Cyr61 provokes cytosolic accumulation of the cell cycle inhibitor p21$^{Cip1/WAF1}$ through activation of the PI-3K/Akt/GSK3β signaling cascade

CCN proteins are known to stimulate Akt signaling through interaction with integrins that results in integrin-linked kinase-mediated Akt-activating and downstream GSK3β-inactivating phosphorylation. Targets of this Akt signaling cascade include the cell cycle regulators p21$^{Cip1/WAF1}$, p27, and Cyclin D1. Thus, we hypothesized that Cyr61 overexpressed in SaOS-2/Cyr61 cells might activate the described cascade and thereby stimulate the growth of tumors and metastases. hrCyr61 indeed stimulated the phosphorylation of Akt at Ser473 in serum-starved SaOS-2 cells in a dose- and time-dependent manner (Fig. 5*A–D*). A maximal 7.5-fold increase of phospho-Akt in response to 200 ng/mL hrCyr61 was observed after 30 minutes (Fig. 5*B, D*). The hrCyr61-stimulated phosphorylation of Akt and of its downstream target GSK3β at Ser9 was suppressed in the presence of 100 μM PI-3K inhibitor LY294002 (Fig. 5*E*), indicating PI-3K-mediated Akt activation by hrCyr61. Moreover, preincubation and stimulation of SaOS-2 cells with hrCyr61 in the presence of an integrin Arg-Gly-Asp (RGD)–domain blocking peptide or αVβ3 or αVβ5 integrin blocking antibodies also inhibited Akt phosphorylation and confirmed integrin-mediated signaling of hrCyr61 in SaOS-2 cells (Supplemental Fig. S1). The levels of the cell cycle inhibitor p27 in SaOS-2 cell extracts remained unchanged after stimulation with 200 ng/mL hrCyr61 for 30 minutes (not shown), but, interestingly, an accumulation of p21$^{Cip1/WAF1}$ and of Cyclin D1 in total cell lysates was observed (Fig. 5*E*).

This finding was further investigated by analyzing the nuclear and cytoplasmic levels of p21$^{Cip1/WAF1}$ before and after incubation of serum-starved SaOS-2 cells with 200 ng/mL hrCyr61 for 30 minutes. Interestingly, p21$^{Cip1/WAF1}$ accumulated in the cytoplasmic fraction of stimulated cells (Fig. 5*E*). This finding was confirmed by predominant nuclear p21$^{Cip1/WAF1}$ immunofluorescent staining in nonstimulated cells and pronounced cytoplasmic staining in cells stimulated with 200 ng/mL

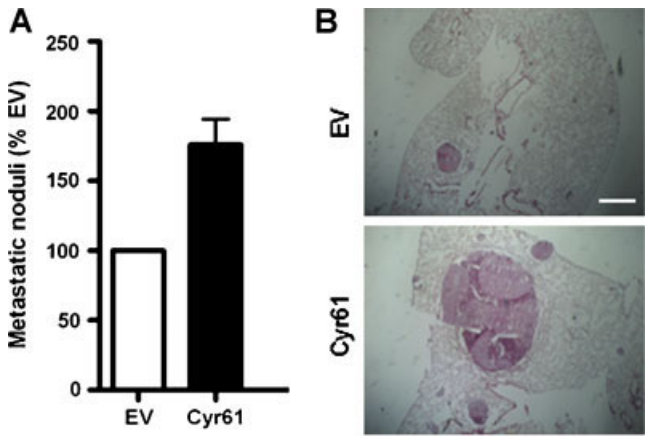

Fig. 4. Cyr61 overexpression in SaOS-2 osteosarcoma cells promotes lung metastasis in SCID mice. (*A*) Percent metastatic lesions in lungs of mice injected with SaOS-2/Cyr61 cells (Cyr61) normalized to the number of lung lesions in mice injected with SaOS2/EV cells (EV) set to 100%. Data are the mean ± SEM collected from five mice per group. (*B*) Representative images of HE-stained lung sections of mice injected with SaOS2/EV cells (top) or with SaOS-2/Cyr61 cells (bottom). Metastases appear as dense HE-stained areas. Scale bars = 200 μm.

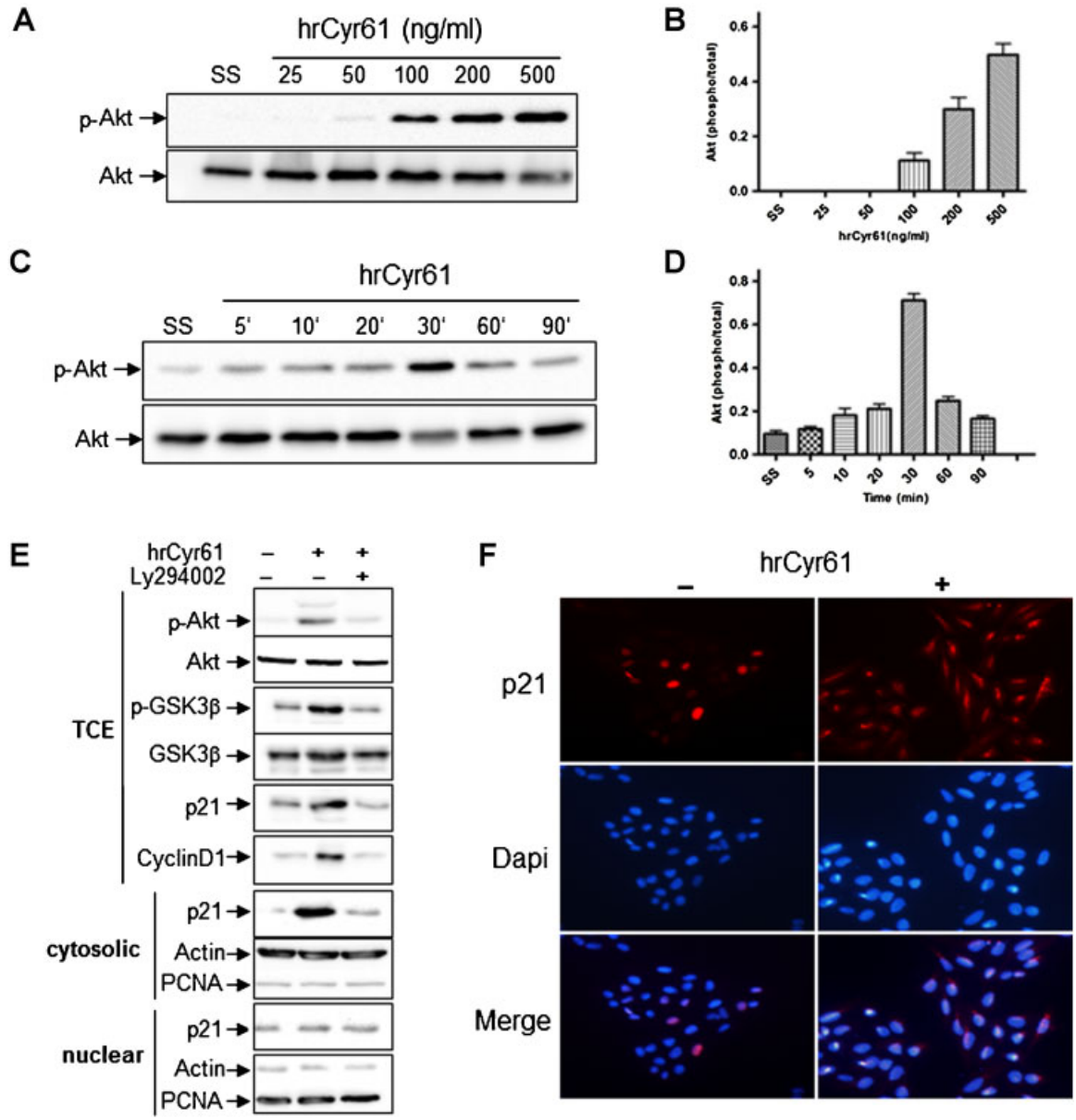

Fig. 5. Cyr61 stimulates Akt/GSK3β signaling in SaOS-2 cells dose- and time-dependently through activation of phosphatidylinositol 3′-kinase (PI-3K) and provokes cytoplasmic accumulation of the cell cycle inhibitor p21. Representative Western blots (*A, C, E*) of total cell extracts (TCE) or of cytosolic (cytosolic) or nuclear (nuclear) fractions of serum-starved cells stimulated with indicated concentrations of recombinant human rhCyr61 for 30 minutes (*A*) or with 200 ng/mL rhCyr61 for indicated time periods (*C*) or with 200 ng/mL rhCyr61 for 30 minutes in the absence (−) or in the presence (+) of 100 μM PI-3K inhibitor LY294002 (*E*). Blots were analyzed with antibodies to phospho-Ser^{473}-Akt (p-Akt), Akt, phospho-Ser^{9}-GSK3β (p-GSK3β), GSK3β, p21$^{Cip1/WAF1}$ (p21), Cyclin D1, actin, and PCNA as indicated. Quantitative analysis of Western blots of three independent rhCyr61 dose-response (*B*) or time-course (*D*) experiments. Data indicate mean (±SEM) levels of p-Akt normalized to total Akt in individual protein extracts. (*F*) Predominant nuclear or cytoplasmic localization of immunofluorescent p21 (red) in SaOS-2 cells incubated in the absence (−) or in the presence (+) of 200 ng/mL rhCyr61 for 30 minutes. Nuclei (blue) were stained with 4,6-diamidino-2-phenylindole (DAPI).

hrCyr61 for 30 minutes (Fig. 5*F*). Thus, Cyr61 provokes subcellular redistribution in SaOS-2 cells through activation of the integrin-PI-3K/Akt/GSK3β signaling cascade.

Discussion

Despite sophisticated surgical techniques used for the resection of primary osteosarcoma tumors and significant progress in neoadjuvant chemotherapy over the last three decades, patients with metastasizing osteosarcoma or recurrent disease continue to have a poor prognosis with less than 20% mean 5-year survival.[4–6] In addition, 25% to 50% of osteosarcoma patients, who at the time of diagnosis present with local disease, subsequently develop metastases. Consequently, reliable molecular markers for early diagnosis of metastatic osteosarcoma and more detailed knowledge on key mechanisms in the metastatic process are crucial for more effective treatment of osteosarcoma patients with new drugs that target metastasizing tumor cells at an early stage.

The current study therefore focused on the identification of novel candidate marker proteins that, when expressed in osteosarcoma primary tumors, activate cellular processes that enforce the metastatic phenotype and consequently are indicators of high aggressiveness and poor prognosis. The Kaplan-Meier survival analysis presented here revealed a significant correlation between Cyr61 expression in osteosarcoma primary tumors and poor prognosis for the patients, irrespective of metastatic or nonmetastatic disease. The analysis also confirmed the long-documented clinical observation that mortality of osteosarcoma patients correlates with metastasis of the primary tumor. Moreover, the findings reported here are in good agreement with the results reported by Fromigue and colleagues,[30] who demonstrated that the expression of Cyr61, assessed by immunohistochemistry in tumor tissue, correlated with osteosarcoma tumor grade. However, the findings reported here and by Fromigue and colleagues are different from the results described by Perbal and colleagues,[34] who analyzed Cyr61 expression in osteosarcoma tissue at the mRNA level by quantitative RT-PCR and found no correlation of Cyr61 expression and malignancy of the tumor. A likely higher stability of proteins than of mRNA in osteosarcoma tissue specimens may account for the discrepant results obtained by quantitative RT-PCR and immunohistochemistry. Based on the results reported here and on comparable findings in other cancer types,[35,36] we hypothesized that Cyr61, when expressed in osteosarcoma, has tumorigenic- and metastasis-promoting activity. This hypothesis was indeed corroborated in the here reported intratibial xenograft osteosarcoma mouse model, in which the well-established low-metastatic human SaOS-2 osteosarcoma cell line[37] and a modified Cyr61-overexpressing SaOS-2/Cyr61 subline were used. In this osteosarcoma mouse model that reproduced the life-threatening condition in humans, SaOS-2/Cyr61 cells showed a markedly enhanced malignant phenotype compared with SaOS-2/EV control cells. This was reflected in accelerated primary tumor growth, a higher density of lung metastatic foci with a higher percentage of macrometastases, and, consequently, a significantly shorter survival of the mice injected with SaOS-2/Cyr61 cells compared with the animals that received SaOS-2/EV control cells. These observations were remarkably consistent with the working hypothesis and, moreover, in good agreement with the results recently reported by Fromigue and colleagues,[30] who used an intramuscular mouse osteosarcoma model that less precisely reproduced the human disease than the intratibial human xenograft model in the current study. Nevertheless, Fromigue and colleagues also demonstrated a malignancy-promoting activity of Cyr61 in osteosarcoma, which when downregulated, resulted in less-aggressive lung metastasis, consistent with reduced invasive and migratory activity in vitro observed in their and our study.

Cyr61 is known to interact with integrins, which signal through integrin-linked kinase (ILK) to the β-catenin-TCF/Lef signaling pathway and to Akt signaling cascades that they share with receptor tyrosine kinases.[38–41] Moreover, it has been shown that multiple integrins, especially $\alpha_v\beta_3$, were upregulated by Cyr61 protein along with an increase in ILK activity and Akt activation.[42] In the current study, stimulation of SaOS-2 cells with hrCyr61 resulted in time- and dose-dependent phosphorylation of Akt through PI-3K, mediated by αVβ3 and αVβ5 integrins, and, consequently, downstream phosphorylation of GSK3β increased Cyclin D1 levels and cytosolic accumulation of the cell cycle inhibitor $p21^{Cip1/WAF1}$. Interestingly, the cellular levels of the other cell cycle inhibitor, p27, also targeted by phosphorylated GSK3β, remained unchanged after stimulation of SaOS-2 cells with hrCyr61, and nuclear translocation of β-catenin, a readout of the β-catenin-TCF/Lef signaling pathway, was also not observed. Subcellular relocalization of $p21^{Cip1/WAF1}$, mediated by Akt signaling as reported here, has also been described in a previous study on breast cancer, which demonstrated that phospho-Akt promoted cell growth in Her2/neu-overexpressing cells.[43] A significant stimulation of cell proliferation by hrCyr61 in SaOS-2 cells in culture was not evident in the current study, but in vivo, overexpression of Cyr61 in SaOS-2/Cyr61 cells promoted intratibial primary tumor growth significantly.

Based on the findings of this study and the reported biological properties of Cyr61 as an extracellular matrix-associated ligand of several integrins,[13,44–46] auto- and paracrine integrin-mediated Cyr61 signaling must be considered as a likely mechanism that activates cellular programs in osteosarcoma primary tumor cells required for dissemination to metastatic sites and outgrowth of the metastasizing cell in the new tissue environment. This proposed mechanism of action of Cyr61, when upregulated in osteosarcoma primary tumors, is in line with previously described signaling functions of integrins in the regulation of cell migration, invasion, and proliferation.[47,48] Apparently, in the animal model reported here, constitutively elevated production of Cyr61 by SaOS-2/Cyr61 cells maintains in the local environment of the developing intratibial tumor and of lung metastases concentrations of the protein that are sufficient for continuous integrin-mediated signaling of Cyr61 to downstream stimulatory regulators of tumor growth and metastasis.

In conclusion, the current findings revealed Cyr61 as a novel indicator for poor prognosis in osteosarcoma similar to ezrin, the most extensively investigated marker in osteosarcoma. It is conceivable that Cyr61 in concert with ezrin, which has been postulated as a coordinator and amplifier of cell surface signals, could act as metastasis-promoting effectors when aberrantly overexpressed in osteosarcoma, and this remains fertile ground for future investigation. Finally, our study identifies Cyr61 and the integrin-Akt signaling axis as potential new targets to be considered for more effective treatment of osteosarcoma patients.

Disclosures

All the authors state that they have no conflicts of interest.

Acknowledgments

We thank Dr S Gery (Cedars-Sinai Medical Center, Los Angeles, CA, USA) for providing a pcDNA3-Myc/Cyr61 plasmid. We thank Dr J Snedeker (Orthopedic Biomechanics, University of Zurich/ETH, Zurich, Switzerland) for reading the manuscript.

This work was supported by the Swiss National Science Foundation (SNF grant number 31003A-120403), a grant from the Zurcher Krebsliga (Zurich, Switzerland), the University of Zurich, and the Schweizerischer Verein Balgrist (Zurich, Switzerland), the Walter L. & Johanna Wolf Foundation (Zurich, Switzerland) as well as the Lydia Hochstrasser Stiftung (Zurich, Switzerland).

Authors' roles: AAS: project leader; MJEA: animal work; RM: tissue culture; BB: collection and analysis of tumor tissue specimens, generation of tissue microarray; BL: technical assistance; JB: technical assistance; TJ: analysis of tissue microarray: GJP: analysis of tissue microarray; WB: study design and manuscript editing; BF: study design and manuscript editing.

References

1. Fuchs B, Pritchard DJ. Etiology of osteosarcoma. Clin Orthop Relat Res. 2002;397:40–52.
2. Kager L, Zoubek A, Potschger U, et al. Primary metastatic osteosarcoma: presentation and outcome of patients treated on neoadjuvant Cooperative Osteosarcoma Study Group protocols. J Clin Oncol. 2003;21:2011–8.
3. Mialou V, Philip T, Kalifa C, et al. Metastatic osteosarcoma at diagnosis: prognostic factors and long-term outcome—the French pediatric experience. Cancer. 2005;104:1100–9.
4. Gorlick R, Meyers PA. Osteosarcoma necrosis following chemotherapy: innate biology versus treatment-specific. J Pediatr Hematol Oncol. 2003;25:840–1.
5. Hawkins DS, Arndt CA. Pattern of disease recurrence and prognostic factors in patients with osteosarcoma treated with contemporary chemotherapy. Cancer. 2003;98:2447–56.
6. Klein MJ, Siegal GP. Osteosarcoma: anatomic and histologic variants. Am J Clin Pathol. 2006;125:555–81.
7. Khanna C, Wan X, Bose S, et al. The membrane-cytoskeleton linker ezrin is necessary for osteosarcoma metastasis. Nat Med. 2004;10: 182–6.
8. Khanna C, Hunter K. Modeling metastasis in vivo. Carcinogenesis. 2005;26:513–23.
9. Park HR, Jung WW, Bacchini P, et al. Ezrin in osteosarcoma: comparison between conventional high-grade and central low-grade osteosarcoma. Pathol Res Pract. 2006;202:509–15.
10. Gorlick R, Khanna C. Osteosarcoma. J Bone Miner Res. 2010;25: 683–91.
11. Kireeva ML, Mo FE, Yang GP, et al. Cyr61, a product of a growth factor-inducible immediate-early gene, promotes cell proliferation, migration, and adhesion. Mol Cell Biol. 1996;16:1326–34.
12. Babic AM, Kireeva ML, Kolesnikova TV, et al. CYR61, a product of a growth factor-inducible immediate early gene, promotes angiogenesis and tumor growth. Proc Natl Acad Sci USA. 1998;95:6355–60.
13. Kireeva ML, Lam SC, Lau LF. Adhesion of human umbilical vein endothelial cells to the immediate-early gene product Cyr61 is mediated through integrin alphavbeta3. J Biol Chem. 1998;273: 3090–6.
14. Kolesnikova TV, Lau LF. Human CYR61-mediated enhancement of bFGF-induced DNA synthesis in human umbilical vein endothelial cells. Oncogene. 1998;16:747–54.
15. Lau LF, Lam SC. The CCN family of angiogenic regulators: the integrin connection. Exp Cell Res. 1999;248:44–57.
16. Chen CC, Lau LF. Functions and mechanisms of action of CCN matricellular proteins. Int J Biochem Cell Biol. 2009;41:771–83.
17. Xie D, Nakachi K, Wang H, et al. Elevated levels of connective tissue growth factor, WISP-1, and CYR61 in primary breast cancers associated with more advanced features. Cancer Res. 2001;61:8917–23.
18. Xie D, Miller CW, O'Kelly J, et al. Breast cancer. Cyr61 is overexpressed, estrogen-inducible, and associated with more advanced disease. J Biol Chem. 2001;276:14187–94.
19. Jiang WG, Watkins G, Fodstad O, et al. Differential expression of the CCN family members Cyr61, CTGF and Nov in human breast cancer. Endocr Relat Cancer. 2004;11:781–91.
20. Xie D, Yin D, Wang HJ, et al. Levels of expression of CYR61 and CTGF are prognostic for tumor progression and survival of individuals with gliomas. Clin Cancer Res. 2004;10:2072–81.
21. Sin WC, Bechberger JF, Rushlow WJ, et al. Dose-dependent differential upregulation of CCN1/Cyr61 and CCN3/NOV by the gap junction protein Connexin43 in glioma cells. J Biol Chem. 2008;103:1772–82.
22. Bleau AM, Planque N, Perbal B. CCN proteins and cancer: two to tango. Front Biosci. 2005;10:998–1009.
23. Gery S, Xie D, Yin D, et al. Ovarian carcinomas: CCN genes are aberrantly expressed and CCN1 promotes proliferation of these cells. Clin Cancer Res. 2005;11:7243–54.
24. Tong X, Xie D, O'Kelly J, et al. Cyr61, a member of CCN family, is a tumor suppressor in non-small cell lung cancer. J Biol Chem. 2001;276:47709–14.
25. Chien W, Kumagai T, Miller CW, et al. Cyr61 suppresses growth of human endometrial cancer cells. J Biol Chem. 2004;279:53087–96.
26. Chen PP, Li WJ, Wang Y, et al. Expression of Cyr61, CTGF, and WISP-1 correlates with clinical features of lung cancer. PloS One. 2007;2:e534.
27. Maeta N, Osaki M, Shomori K, et al. CYR61 downregulation correlates with tumor progression by promoting MMP-7 expression in human gastric carcinoma. Oncology. 2007;73:118–26.
28. Lin MT, Kuo IH, Chang CC, et al. Involvement of hypoxia-inducing factor-1alpha-dependent plasminogen activator inhibitor-1 upregulation in Cyr61/CCN1-induced gastric cancer cell invasion. J Biol Chem. 2008;283:15807–15.
29. Watari H, Xiong Y, Hassan MK, et al. Cyr61, a member of ccn (connective tissue growth factor/cysteine-rich 61/nephroblastoma overexpressed) family, predicts survival of patients with endometrial cancer of endometrioid subtype. Gynecol Oncol. 2009;112:229–34.
30. Fromigue O, Hamidouche Z, Vaudin P, et al. Cyr61 downregulation reduces osteosarcoma cell invasion, migration and metastases. J Bone Miner Res. 2011;26:1533–42.
31. Fletcher CDM, Unni KK, Mertens F, eds. World Health Organization classification of tumours. Pathology and genetics of tumours of soft tissue and bone. Lyon, France: IARC Press; 2002.
32. Kononen J, Bubendorf L, Kallioniemi A, et al. Tissue microarrays for high-throughput molecular profiling of tumor specimens. Nat Med. 1998;4:844–7.
33. Graham FL, van der Eb AJ. A new technique for the assay of infectivity of human adenovirus 5 DNA. Virology. 1973;52:456–67.
34. Perbal B, Zuntini M, Zambelli D, et al. Prognostic value of CCN3 in osteosarcoma. Clin Cancer Res. 2008;14:701–9.
35. Dhar A, Ray A. The CCN family proteins in carcinogenesis. Exp Oncol. 2010;32:2–9.
36. D'Antonio KB, Schultz L, Albadine R, et al. Decreased expression of Cyr61 is associated with prostate cancer recurrence after surgical treatment. Clin Cancer Res. 2010;16:5908–13.
37. Jia SF, Worth LL, Kleinerman ES. A nude mouse model of human osteosarcoma lung metastases for evaluating new therapeutic strategies. Clin Exp Metastasis. 1999;17:501–6.
38. Delcommenne M, Tan C, Gray V, et al. Phosphoinositide-3-OH kinase-dependent regulation of glycogen synthase kinase 3 and protein kinase B/AKT by the integrin-linked kinase. Proc Natl Acad Sci USA. 1998;95:11211–6.

39. Sonoda Y, Watanabe S, Matsumoto Y, et al. FAK is the upstream signal protein of the phosphatidylinositol 3-kinase-Akt survival pathway in hydrogen peroxide-induced apoptosis of a human glioblastoma cell line. J Biol Chem. 1999;274:10566–70.
40. Dedhar S, Williams B, Hannigan G. Integrin-linked kinase (ILK): a regulator of integrin and growth-factor signalling. Trends Cell Biol. 1999;9:319–23.
41. Persad S, Attwell S, Gray V, et al. Regulation of protein kinase B/Akt-serine 473 phosphorylation by integrin-linked kinase: critical roles for kinase activity and amino acids arginine 211 and serine 343. J Biol Chem. 2001;276:27462–9.
42. Xie D, Yin D, Tong X, et al. Cyr61 is overexpressed in gliomas and involved in integrin-linked kinase-mediated Akt and beta-catenin-TCF/Lef signaling pathways. Cancer Res. 2004;64:1987–96.
43. Zhou BP, Liao Y, Xia W, et al. Cytoplasmic localization of p21Cip1/WAF1 by Akt-induced phosphorylation in HER-2/neu-overexpressing cells. Nat Cell Biol. 2001;3:245–52.
44. Jedsadayanmata A, Chen CC, Kireeva ML, et al. Activation-dependent adhesion of human platelets to Cyr61 and Fisp12/mouse connective tissue growth factor is mediated through integrin alpha(IIb)beta(3). J Biol Chem. 1999;274:24321–7.
45. Chen CC, Chen N, Lau LF. The angiogenic factors Cyr61 and connective tissue growth factor induce adhesive signaling in primary human skin fibroblasts. J Biol Chem. 2001;276:10443–52.
46. Grzeszkiewicz TM, Kirschling DJ, Chen N, et al. CYR61 stimulates human skin fibroblast migration through Integrin alpha vbeta 5 and enhances mitogenesis through integrin alpha vbeta 3, independent of its carboxyl-terminal domain. J Biol Chem. 2001;276:21943–50.
47. Giancotti FG, Ruoslahti E. Integrin signaling. Science. 1999;285:1028–32.
48. Ruoslahti E. Fibronectin and its integrin receptors in cancer. Adv Cancer Res. 1999;76:1–20.